Materials Sciences and Applications, 2023, 14, 382-396
https://www.scirp.org/journal/msa
ISSN Online: 2153-1188
ISSN Print: 2153-117X

Thermal Effect of Braking on Pavements during Heat Waves in Ouagadougou

Sidpouita Mathilde Koudougou[1,2], Hamma Fabien Yonli[2,3], Moussa Sougoti[2,4], David Yemboini Kader Toguyeni[1,2]

[1]Institut du Génie des Systèmes Industriels de Textiles, Ecole Polytechnique de Ouagadougou, Ouagadougou, Burkina Faso
[2]Laboratoire de Physique et de Chimie de l'Environnement, Ouagadougou, Burkina Faso
[3]Université de Fada N'Gourma, Fada N'Gourma, Burkina Faso
[4]Université Joseph Ki-Zerbo, Ouagadougou, Burkina Faso
Email: koudougoumathilde@yahoo.fr

How to cite this paper: Koudougou, S.M., Yonli, H.F., Sougoti, M. and Toguyeni, D.Y.K. (2023) Thermal Effect of Braking on Pavements during Heat Waves in Ouagadougou. *Materials Sciences and Applications*, **14**, 382-396.
https://doi.org/10.4236/msa.2023.147024

Received: May 26, 2023
Accepted: July 15, 2023
Published: July 18, 2023

Abstract

Flexible pavements, whose surface layers are made from hot mix asphalt, may show rutting in some of these infrastructures during the first months of life. In the city of Ouagadougou, this rutting phenomenon is sometimes observed. The objective of this article is to quantify the thermal response of the wearing course of national roads 1 and 2, when they are subjected to the braking of heavy trucks of 13 tons and 20 tons per axle. The meteorological conditions retained are those of the Burkinabe climate. The evaluation of the temperature was carried out by numerical simulation using the Comsol Multiphysics 5.2 software. This study showed that the thermal response of the pavement to the combined effects of surface temperature, overloading by a 20 tons heavy truck and braking during a heat wave increase in pavement surface temperature ranging from 1.09% for National Road 1 to 0.91% for National Road 2, particularly in the braking zone. This made it possible to establish the diagnosis according to which the nature of the bitumen used on the wearing course can reduce rigidity modulus. In predictive terms, they allowed us to deduce that an under-dimensioning of the wearing course, even if the bitumen was used is adequate.

Keywords

Road, Modeling, Finite Elements, Thermomechanical, Tropical Climate

1. Introduction

The construction of a durable pavement in a dry tropical zone confronted with the importance of temperature cycle variations during the day. They can reach up to 20.4˚C in the dry season for the city of Ouagadougou. It is necessary to consider this in the design and formulation of road materials.

In terms of pavement life cycle assessment, traffic is considered as one of the main factors of pavement deterioration. Tangential surface stresses generate friction from vehicle wheels on the wearing course, which increases the potential damage of the layer. Cracking of the pavement surface as well as rutting can be observed [1] [2]. The work of Wang *et al.* [3] showed, for example, that tire braking due to increased shear strains increased the rutting of the wearing course by 2 to 2.6 times.

Depending on their magnitude, ruts can be indicative of structural or pavement design failures that pose significant challenges for recycling or even reconstruction of the road infrastructure.

Weather and traffic conditions are taken into account in pavement design through the notion of equivalent temperature in order to achieve the desired life cycle of road infrastructures. Unfortunately, more and more deformations are observed, particularly during heat waves, on certain road infrastructures in the city of Ouagadougou.

In the dry tropical weather conditions of Burkina Faso, during a heat wave, the temperature at the surface of the pavement can reach 62˚C [4]. According to the work of [5], this temperature is conducive surely to adhesion failures at the bitumen/aggregate interfaces. Moreover, it is higher than the critical temperature of 60˚C, defined by the ageing requirements for bitumen [6].

The design stage, which precedes the construction of a bituminous pavement, also requires the Young's modulus values of the pavement layers in order to evaluate its service life. The thermal sensitivity of the moduli of the asphalt layers is not taken into account for temperatures above 45˚C by the sizing software such as Alizé-LCPC. The mechanical behavior of the layer should be controlled at hot weather conditions because they are vulnerable to distresses such as rutting and cracking. In this paper, the mechanical behavior of the layers will be studied at temperatures beyond the maximum design temperatures under load and overload conditions.

The objective of this paper is to estimate the effect of wheel braking of heavy trucks (13 and 20 tons per axle) on the deformations observed in the braking zones (traffic lights, roundabouts). For this purpose, two pavements of the city of Ouagadougou (national road 1 and national road 2) differing by the geometrical values and the nature of the materials used for the formulation of the pavement layers were studied. The static braking mechanism under extreme heat wave conditions was simulated using Comsol Multiphysics 5.2 software in order to evaluate the values of the temperature that could be observed. A comparative study of the simulated temperature values at the surface of the wearing courses of these pavements with the melting temperatures of the bitumens was carried out for the selected loads.

2. Materials and Methods

Within the framework of this work, the national roads 1 and 2 (NR1 and NR2) of the city of Ouagadougou, were studied. These are the sections located between kilometric points KP2+675 and KP2+850, with a length of 175 meters for the NR1; and kilometric points PK00 and PK00+275, with a length of 275 meters for the NR2. The NR1 is located to the west of the city and can be identified by the following geographical coordinates N 12.34359˚, W 001.56948˚. The NR2 is located to the north of the city of Ouagadougou with the following geographical coordinates N 12.38836˚, W 001.48810˚. From a geotechnical point of view, both pavements are flexible and made up of four (4) layers: a wearing course and a base course in bituminous mix, a sub-base course above the sub-base.

The different materials of the pavement layers were reconstituted in the laboratory from the formulas used by road builders.

2.1. Materials

2.1.1. Bitumen

The pure bitumen 50/70 and modified 10/65 bitumens were used in the design of the surface courses. The characteristics of these bitumens are listed in **Table 1**.

The asphalt mixes used in the wearing course and the base course are composed of a mixture of crushed granite and bitumen. The granites used for the asphalt mixes of the two pavements come from different quarries. The granites for the NR1 are from the Yimdi quarry, located at N 12.30098˚, W 001.69862˚ and those for the NR2, from the Yagma quarry, located at N 12.38555˚, W 001.55814˚.

2.1.2. Sub-Base Course and Soil Subgrade

The sub-base is obtained by lithostabilization [7].

The Lithostab (LITHO) used in this work is a mixture of 30% crushed granites and lateritic clayey gravels (LGC) from Yimdi at N 12.31131˚, W 001.65680˚ for NR1 and from Banogo at 12˚18'14" for NR2. The subgrade is exclusively composed of the same gravelly clayey lateritic material.

2.2. Methods

The pavement is often considered in the literature as a semi-infinite, isotropic, linear, low-temperature viscoelastic, water-impermeable homogeneous solid medium [8]. It is not expected to produce energy translated into zero internal heat flux (zero geothermal gradient) [9]. It is subject to local weather conditions.

Braking mechanisms develop energies at the wheel/road contact surfaces especially during braking. They result from longitudinal and transverse forces of contact of the vehicle with the rough road surface.

Table 1. Bitumen identification. AC or Asphalt Concrete, BC or Grave bitumen, LITHO or Lithostab, LGC or LateriticClayey Gravels.

Layer	Bitumen grade	ρ (kg/m^3)	Penetrability (˚C)	BRT (˚C)
AC and BC NR1	50/70	1025	38.66	54.75
AC-NR2	10/65	1.026	27.16	65.5

The proposed linear thermoelastic numerical model can be represented schematically as shown in **Figure 1**.

The physical problem posed in this article couples heat transfer and mechanical loading phenomena.

2.2.1. Formulation of Heat Transfer Phenomena

The equation governing the heat transfer in the different layers of the pavement is given by:

$$\Delta T = \frac{1}{k}\frac{\partial T}{\partial t} \quad (1)$$

Where T is the temperature and D the thermal diffusivity.

The transfer phenomena that come into play are heat conduction in the different layers of the pavement, natural convection from the wind and heat deposited on the pavement surface from braking mechanisms on the wearing course.

1) Energy balance in the pavement

The pavement is subject to weather and traffic conditions. Under these conditions, the net energy φ_{net} (W/m^2) available at its surface which is then transferred by conduction to the different layers is given by the following relation [10]:

$$\varphi_{net} = \varphi_a + \varphi_r + \varphi_{cond} + \varphi_{conv} + \varphi_{braking} \quad (2)$$

φ_a : energy absorbed by the pavement from direct solar radiation;

φ_r : energy emitted from the pavement to the sky;

φ_{cond} : energy transferred to the pavement by conduction;

φ_{conv} : energy transferred to the pavement by convection.

There are two components to solar radiation incident on the pavement surface:

The sun emits short-wave radiation onto the pavement surface. Part of its energy is absorbed by the pavement surface causing a rise in the pavement temperature. This energy is given by:

$$\varphi_a = (1-\alpha) R_g , \quad (3)$$

where α is the albedo and R_g the global radiation.

In our case, the albedo of the road surface is equal to 0.18 [8].

The pavement in turn emits long wave radiation to the sky according to the Stefan-Boltzmann law:

$$\varphi_r = \sigma\epsilon\left(T_{sky}^4 - T_s^4\right) \quad (4)$$

with σ is the Boltzmann constant, ϵ the emissivity of the pavement surface, T_{sky} sky temperature, T_s the temperature at the surface of the pavement, ϵ The emissivity of the pavement surface is taken equal to 0.92 [8];

The sky temperature is given by [11]:

$$T_{sky} = 94.12\ln\left(P_v\right) - 13I_c + 0.314T_{air} \quad (5)$$

where P_v is the vapor pressure, I_c is the sky clarity index and T_{air} is the air temperature.

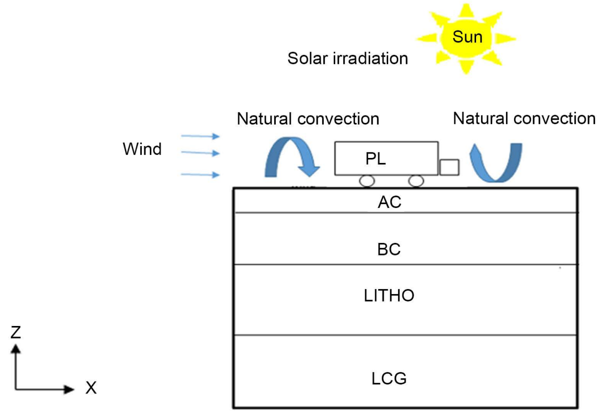

Figure 1. Presentation of the linear thermoelastic model with braking. AC or Asphalt Concrete, BC or Grave bitumen, LITHO or Lithostab, LGC or Lateritic Clayey Gravels.

2) Heat flux transmitted to the pavement by conduction

The energy flow obtained by conduction φ_{cond} at the pavement surface can be approximately calculated by the following relationship [12]:

$$\varphi_{cond} = -k\frac{T_z - T_s}{z} \tag{6}$$

with k the thermal conductivity of the layer, T_z the temperature at depth z.

3) Heat flow generated by convection phenomena

The wearing course is subjected to the phenomena of natural convection. Natural convection is a transfer of energy between the air and the pavement surface.

The convective energy is given by Newton's law:

$$\varphi_{conv} = h_c\left(T_s - T_{air}\right) \tag{7}$$

with h_c the convective exchange coefficient.

The wind speed, V_{wind} of the city of Ouagadougou, is generally below 5 m/s at 30 m from the ground [13], therefore the expression of the convective exchange coefficient [8] [9] is the following

$$h_c = 5.8 + 4.1 \times V_{wind} \tag{8}$$

4) Heat flow generated by the braking process

In general, the empirical braking distance is given by the relation:

$$D_{br} = \frac{v^2}{2g\left(\mu_l + p\right)} \tag{9}$$

where p is the slope of the roadway's longitudinal profile [14].

The energy flow produced by braking is, by deduction:

$$\varphi_{braking} = M\gamma\frac{v^2}{2g\left(\mu_l \pm p\right) \times t_{br} \times S_{br}} \tag{10}$$

where M and v the respective mass and speed of the vehicle, g the acceleration of gravity, μ_l the friction coefficient, t_{br} braking time, S_{br} the braking surface.

5) Mechanical loading

The pavement is also subjected to the weight of the vehicles. We consider two wheels per HT, each carrying half the axle load, *i.e.* 6.5 tons and 10 tons respectively.

6) Strains

The thermal stresses induced by heat transfer and the weight of the truck generate strains in the pavement layers.

These strains ϵ_T on the pavement can be divided into strains induced by thermal stresses ϵ_{th} producing a mechanical response and "pure" mechanical strains ϵ_m, come from the load of the vehicle wheels on the running surface [15].

They are given the following relationship:

$$\epsilon_T = \epsilon_m + \epsilon_{th} = \epsilon_m + \alpha_{th}\Delta T \quad (11)$$

with α_{th} the coefficient of thermal expansion and ΔT the temperature variation at the surface of the layer.

2.2.2. Linear Thermoelastic Model of Pavement Subjected to Braking

The numerical model is built on the finite element method using the Comsol Multiphysics 5.2 software. The input data are the geometrical characteristics of the pavement, the thermophysical and geotechnical properties of the materials, the hourly evolution of the meteorological parameters as well as the braking parameters obtained from the mathematical formula of the problem.

The output parameters are the temperature associated of the wearing course.

1) Initial temperature condition

The initial condition chosen, was obtained by theoretical calculation [4] from the general solution of the heat Equation (1) can take the following real form:

$$T(z,t) = \overline{T} + A_0 \mathrm{e}^{-kz} \sin\left(\omega t - \varphi(z)\right) \quad [16] \quad (12)$$

with A_0 is the daily temperature amplitude;

$$\varphi = kz \quad (13)$$

is the phase;

$$k = \sqrt{\frac{\pi}{D\tau}} \quad (14)$$

is the thermal conductivity.

The results are reported in **Table 2**.

2) Meteorological and geometrical parameters of the model

The meteorological data used for the simulations come from the National Directorate of Meteorology of Burkina Faso.

These are hourly values from 6 am to 6 pm of solar radiation, air temperature, dew point temperature, air humidity, wind speed.

The numerical model built is two-dimensional, it takes into account the thickness and length to be simulated when the pavement is dry.

Table 2. Determined initial temperatures of the different layers.

$\bar{T}$ at 06:00 am	A_0	T_{BB}	T_{GB}	T_{LITHO}	T_{GAL}
23.8˚C	19.5˚C	21.1˚C	15.7˚C	15.6˚C	15.6˚C

The braking time is chosen in the period when the pavement temperature is maximum in order to be the most representative of extreme heat wave conditions.

3) Thermo-physical and geotechnical parameters of the model

The thermal conductivities of the four layers (**Figure 1**) were measured while the other thermo-physical parameters such as the coefficient of thermal expansion and the specific heat capacity were taken from the literature [17] [18].

It should be noted that the stiffness moduli of asphalt concrete are temperature-dependent polynomial functions, chosen at the fixed frequency of 10 Hz.

The moduli of the foundation and subgrade layers are obtained by applying the empirical relations [9]. They are assumed to be temperature invariant.

The geotechnical and thermo-physical properties of the surface layers are listed in **Table 3**.

3. Results

The model presented was simulated under extreme weather conditions. For this purpose, the hottest historical day of the year 2018, which corresponds to April 06, 2018, was chosen.

3.1. Model Validation

Temperatures measured at the pavement surface using an infrared thermometer were compared to simulated temperatures using the sky temperature expression proposed by Aubinet (Aubinet, 1994). The simulated temperatures have the same global aspect as the measured ones with a quadratic error of 2.1˚C (**Figure 2**).

3.2. Model Sensitivity Study

The method used to perform the sensitivity analysis is the Moris method. It consists in identifying the influential parameters beforehand and then classifying them according to their influence [21]. The sensitivity analysis of the linear thermoelastic model coupled to braking was carried out on a heavy truck (HT) of 13 tons per axle for the parameters shown in **Table 4**. The results are reported in **Table 4** with the parameter with the lowest order as the most sensitive parameter. It is deduced that the simulation results are very sensitive to the thermal properties of the materials and less sensitive to the length of the pavement. This allowed to reduce the geometrical dimensions of the numerical model in order to optimize the computation time of the Comsol Multiphysics 5.2 software.

3.3. Thermal Response of the Road to Braking

The braking process of 13 tons or 20 tons HT with an equivalent radius of 12.5

cm with a width of 275 mm takes place from the fourteenth hour (2:00 am) of the historical day of April 06, 2018 (warm day). Braking is simulated at the respective braking times of 1.44 seconds, 1.8 seconds, and 2.25 seconds for speeds of 40 km/h, 50 km/h, and 60 km/h.

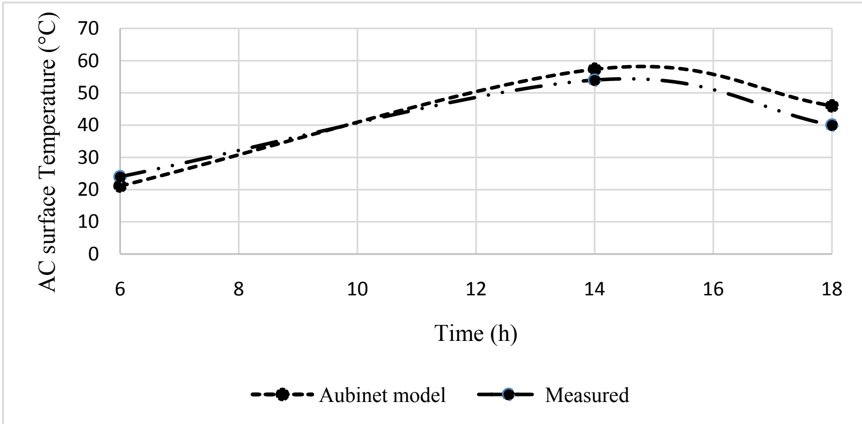

Figure 2. Simulated and measured surface temperatures of the wearing course.

Table 3. Summary table of thermo-physical and geotechnical pavement data. AC or Asphalt Concrete, BC or Grave bitumen, LITHO or Lithostab, LGC or LateriticClayey Gravels.

	Pavement layers	e cm	E Pa	ν	k W/mK	C_p J/kg/˚C	ρ kg/m³	α_{th} µm/m/˚C
NR1	AC	5	$0.1883T^3 + 34.934T^2 + 2151.3T + 4E + 07$	$0.15 + 0.35/\left(1+\exp\left(3.1849 - 0.04233T\left({}^\circ F\right)\right)\right)_a$	1.531	900c	2261	$2 \times 10^{-5}{}_e$
	BC	15	$0.249T^3 + 46.088T^2 + 2829.4T + 6E + 07$	$0.15 + 0.35/\left(1+\exp\left(3.1849 - 0.04233T\left({}^\circ F\right)\right)\right)_a$	1.585	900c	2201	$2 \times 10^{-5}{}_e$
	LITHO	20	1700×10^6	0.4_b	0.77	900d	2150	
	LGC	20	630×10^6	0.4_b	0.67	600d	2120	
NR2	AC	5	$4.2266T^3 + 776.81T^2 - 47325T + 956663$	$0.15 + 0.35/\left(1+\exp\left(3.1849 - 0.04233T\left({}^\circ F\right)\right)\right)_a$	1.747	900c	2310	$2 \times 10^{-5}{}_e$
	BC	12	$1.2248T^3 + 223.28T^2 - 13521T + 272697$	$0.15 + 0.35/\left(1+\exp\left(3.1849 - 0.04233T\left({}^\circ F\right)\right)\right)_a$	1.566	900c	2330	$2 \times 10^{-5}{}_e$
	LITHO	20	4300×10^6	0.4_b	0.77	900d	2140	
	LGC	20	450×10^6	0.4_b	0.67	600d	2120	

a-[17]; b-[18]; c-[19]; d-[9]; e-[20].

Table 4. Results of the sensitivity analysis of the linear thermoelastic model coupled to braking; range of variation of the parameters used for the sensitivity analysis of the linear thermoelastic model coupled to braking.

Input parameter	Range of variation	Sensitivity	Sensitivity level
k	[1.5; 1.6; 1.7]	1.14E-01	2
e	[0.04; 0.05; 0.06]	1.06E-01	3
Lx	[220; 225; 230]	0.00E+00	7
ε	[0.92; 0.90; 0.88]	0.00E+00	7
α	[0.08; 0.10; 0.12]	5.54E-02	4
C_p	[900; 1100; 1200]	2.68E-01	1
p	[0.01; 0.02; 0.03]	3.99E-10	6
μ_l	[0.7; 0.8; 0.9]	3.98E-05	5

The figures showing the simulated pavement surface temperatures before and after braking show an identifiable temperature plateau in the braking zone at all three pavements (**Figures 3-6**).

In the braking zone or over the braking distance, a sudden increase in the temperature of the pavement surface can be observed. The temperatures obtained can reach 66.5˚C. Since this value is much higher than the maximum temperature recorded in the work of [4], it can be stated that braking leads to an increase in the temperature of the pavement surface. Moreover, the maximum temperature of 66.5˚C obtained is well above the critical temperature of 60˚C, defined by the requirements for the ageing of bitumens [6]. One could therefore expect structural disorganization of the asphalt wearing course.

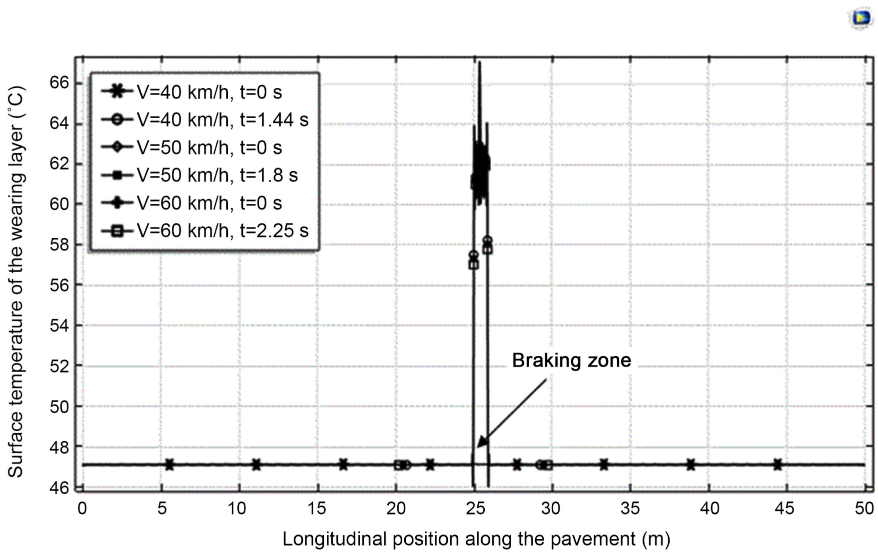

Figure 3. Temperature evolution at the surface of the NR1 for a 13 tons truck travelling at 40 km/h, 50 km/h and 60 km/h.

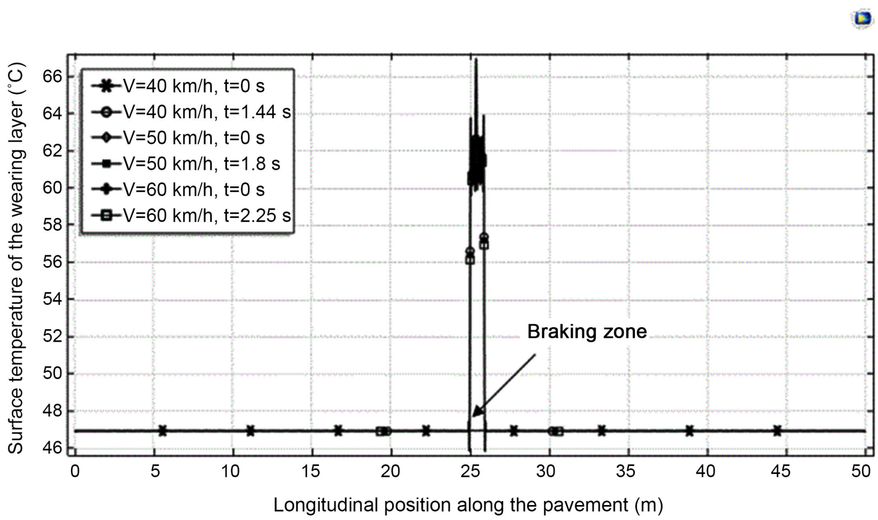

Figure 4. Temperature evolution at the surface of the NR1 for a 20 tons truck travelling at 40 km/h, 50 km/h and 60 km/h.

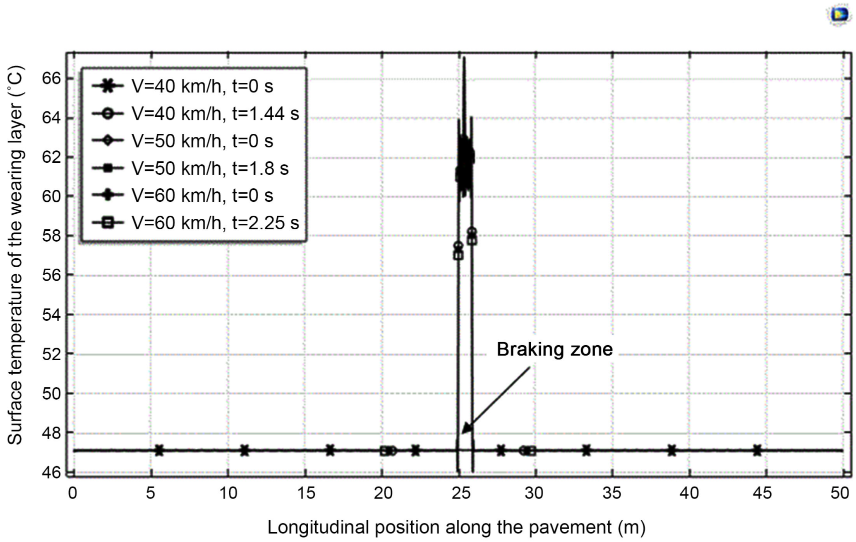

Figure 5. Temperature evolution at the surface of the NR2 for a 13 tons truck travelling at 40 km/h, 50 km/h and 60 km/h.

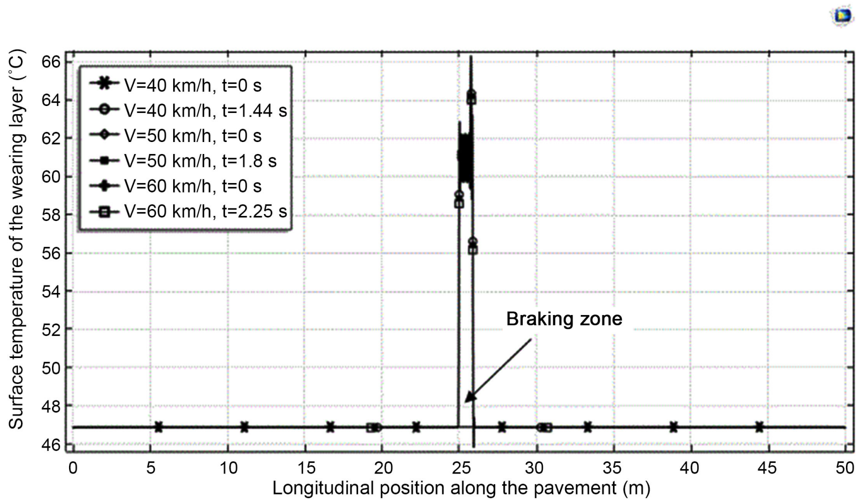

Figure 6. Temperature evolution at the surface of the NR2 for a 20 tons truck travelling at 40 km/h, 50 km/h and 60 km/h.

Furthermore, the temperature rise in the braking zone is weakly proportional to the speed of the vehicle as illustrated in the previous figures (Figures 3-6). As an illustration, a decsrease of 0.1˚C is obtained for a vehicle travelling at 40 km/h compared to a vehicle travelling at 60 km/h on the NR1 for a load of 13 tons.

4. Discussion

The simulations also indicate that the temperature increase in the braking zone is dependent on axle load with an increase of 0.1˚C for a 20 tons truck.

Comparison of simulated pavement surface temperatures in the absence of braking with simulated pavement surface temperatures after braking reveals a significant increase of 1.09% on NR1 and 0.91% on NR2.subjected to a 13 tons HT traveling at 40 km/h (Table 5).

Table 5. Simulated road surface temperatures for 13 tons and 20 tons HT travelling at 40 km/h on NR1 and NR2.

	Axle load	t_{br} (s)	Maximum AC surface temperature (˚C) without braking	Maximum AC surface temperature (˚C) during braking
NR1	13t	1.44	61.5	67.2
	20t	1.44	61.5	67.2
NR2	13t	1.44	60.4	66.4
	20t	1.44	60.4	66.6

Under the overload conditions of a 20 tons truck, the temperature rise at the surface observed on NR1 is 1˚C. This is greater than the 0.6˚C rise on NR2. This would mean that the difference in pavement surface temperature between the 13 tons and 20 tons truck is dependent on the pavement type. As highlighted previously, this difference can double under the same weather conditions depending on the asphalt mix design.

It should also be noted that, in general, the extra load would provide little additional thermal energy compared to the standard 13 tons load (**Table 5**).

The simulated temperature after braking for the wearing course of NR1 is 12.45˚C higher than that of the softening point of the 50/70 bitumen. That of NR2 greater than 1.1˚C relative to the softening point temperature of bitumen 10/65. According to the work of Koudougou and Toguyeni [4], the deformations obtained for these temperatures must be greater than the allowable deformations proposed by the classification diagram of Di Benedetto [22] for T2 traffic.

It is therefore essential during the design of bituminous pavements to make an optimal choice of the grades of bitumen in order to avoid, in the hottest periods of the year, losses of rigidity which would lead to premature deterioration of the pavements.

5. Conclusions

The rutting encountered in the city of Ouagadougou is often subject to speculation. Its origin and prediction are not determined at the National Laboratory of Building and Public Works of Burkina Faso. The objective of this article is to determine the temperature of the wearing course related to the joint effects of braking and dry tropical weather conditions.

The present article has allowed, by means of a numerical approach, to identify the main cause of rutting encountered in a pavement in the city of Ouagadougou. It has been deduced that 50/70 and 10/65 bitumen are not suitable for the design of wearing courses subjected to dry tropical weather conditions. These bitumens have a braking temperature for heavy vehicles of 13 tonnes and 20 tonnes higher than the melting temperatures of the 35/50 and 10/65 bitumens used for the formulation of the surface layers. This could explain an origin linked to the grade of the bitumens in the appearance of the degradations observed in the braking zones.

Acknowledgements

We would like to thank the National Laboratory of Building and Public Works of Burkina Faso for its material and technical support. Our thanks also go to the National Directorate of Meteorology of Burkina Faso.

Conflicts of Interest

The authors declare no conflicts of interest regarding the publication of this paper.

References

[1] Drakos, C., Roque, R. and Birgisson, B. (2001) Effects of Measured Tire Contact Stresses on Near Surface Rutting. *Transportation Research Record*, **1764**, 59-69. https://doi.org/10.3141/1764-07

[2] Al-Qadi, I.L., Wang, H., Yoo, P.J. and Dessouky, S.H. (2008) Dynamic Analysis and *in-situ* Validation of Perpetual Pavement Response to Vehicular Loading. *Transportation Research Record*: *Journal of the Transportation Research Board*, **2087**, 29-39. https://doi.org/10.3141/2087-04

[3] Wang, H. and Al-Qadi, I.L. (2010) Evaluation of Surface-Related Pavement Damage Due to Tire Braking. *Road Materials and Pavement Design*, **11**, 101-121.

[4] Koudougou, S.M. and Toguyeni, D.Y.K. (2020) Modeling of Pavement Behavior in Tropical Hot and Dry Conditions: Numerical Approach and Comparison on Road Section. *Journal of Materials Science & Surface Engineering*, **7**, 919-927.

[5] Cucalon, L.G., Bhasin, A., Kassem, E., Herbert, B.E., Masad, E. and Little, D. (2017) Physicochemical Characterization of Binder-Aggregate Adhesion Varying with Temperature and Moisture. *Journal of Transportation Engineering*, *Part B*: *Pavements*, **143**, Article 04017007. https://doi.org/10.1061/JPEODX.0000001

[6] Bell, C.A. and Sosnovske, D. (1994) Aging: Binder Validation. National Research Council, Washington DC.

[7] Lompo, P. (1980) Les Matériaux Utilisés En Construction Routière En Haute-Volta, Un Matériau Non Traditionnel. *Le Lithostab*, *Irf Ive Conference Routiere Africaine*, 20-25 Janvier 1980, Nairobi, 29-40.

[8] Asfour, S. (2017) Récupération d'énergie dans les chaussées pour leur maintien hors gel. Master's Thesis, Université Blaise Pascal Clermont, Clermont-Ferrand.

[9] Hall, M.R., Dehdezi, P.K., Dawson, A.R., Grenfell, J. and Isola, R. (2012) Influence of the Thermophysical Properties of Pavement Materials on the Evolution of Temperature Depth Profiles in Different Climatic Regions. *Journal of Materials in Civil Engineering*, **24**, 32-47. https://doi.org/10.1061/(ASCE)MT.1943-5533.0000357

[10] Sheeba, J.B. and Rohini, A.K. (2014) Structural and Thermal Analysis of Asphalt Solar Collector Using Finite Element Method. *Journal of Energy*, **2014**, Article ID: 602087. https://doi.org/10.1155/2014/602087

[11] Aubinet, M. (1994) Longwave Sky Radiation Parameterizations. *Solar Energy*, **53**, 147-154. https://doi.org/10.1016/0038-092X(94)90475-8

[12] Solaimanian, M. and Kennedy, T.W. (1993) Predicting Maximum Pavement Surface Temperature Using Maximum Air Temperature and Hourly Solar Radiation. *Journal of the Transportation Research Board*, **1417**, 1-11.

[13] Landry, M., Ouedraogo, Y., Gagnon, Y. and Ouedraogo, A. (2011) Atlas Éolien Du

Burkina Faso. Geography, p. 18.
https://www.semanticscholar.org/paper/Atlas-%C3%A9olien-du-Burkina-Faso-Ou%C3%A9draogo-Landry/524a53e97cc35f9cb0d4360e5a661757e7e3f9c2#citing-papers

[14] Michelin (2011) Adhérence du pneu. Société de technologie Michelin.

[15] Di Benedetto, H. and Neifar, M. (1997) Coefficients de dilatation et de contraction thermiques d'un enrobé bitumineux avec et sans chargement Mécanique, Mechanical Tests for Bituminous Materials. *Proceeding of the* 5*th International Rilem Symposium*, Lyon, 14-16 May 1997, 421-428.

[16] Carslaw, M.S. and Jaeger, J.C. (1954) Conduction of Heat in Solids. Oxford Science Publications, Oxford.

[17] Maher, A. and Bennert, T.A. (2008) Evaluation of Poisson's Ratio for Use in the Mechanistic Empirical Pavement Design Guide (Mepdg). Department of Civil & Environmental Engineering Center for Advanced Infrastructure & Transportation (CAIT) Rutgers, The State University Piscataway, Final Report.

[18] Mirza, M.W. (1999) Development of Relationships to Predict Poisson's Ratio for Paving Materials. Interteam Technical Report for Nchrp, University of Maryland, College Park.

[19] Highter, W.H. and Wall, D.J. (1984) Thermal Properties of Some Asphaltic Concrete Mixes. *Transportation Research Record*, **968**, 38-45.
https://doi.org/10.2514/6.1983-1598

[20] Olard, F. (2003) Comportement thermomécanique des enrobés bitumineux à basses températures. Relations entre les propriétés du liant et de l'enrobé. Master's Thesis, Institut National Des Sciences Appliquées de Lyon, Villeurbanne.

[21] Morris, M.D. (1991) Factorial Sampling Plans for Preliminary Computational Experiments. *Technometrics*, **33**, 161-174.
https://doi.org/10.1080/00401706.1991.10484804

[22] Di Benedetto, H. (1990) Nouvelle approche du comportement des enrobés bitumineux: Résultats expérimentaux et formulation rhéologique. Mechanical tests for bituminous mixes, characterization, design and quality control. *Proceedings of the* 4*th Rilem Symposium*, Budapest, 23-25 October 1990, 387-401.

Abbreviations

NR1: National Road 1

NR2: National Road 2

KP: Kilometric point

AC: Asphalt Concrete

BC: Grave bitumen

LITHO: Lithostab

LGC: Lateritic Clayey Gravels

HT: Heavy Truck

BRT: Ball Ring Temperature

Nomenclature

ϵ_T : total strains

C_p : Heat capacity (J·kg^{-1}·K^{-1})

h_c : Convective exchange coefficient

I_c : Sky clarity index

P_v : Vapor partial pressure (Pa)

R_g : Incident solar radiation (W/m^2)

$\overline{T}$: Hourly average air temperature (˚C)

T_{air} : Température de l'air (˚C)

T_s : Air temperature (˚C)

T_{sky} : Sky temperature (˚C)

T_z : Temperature at depth z (m)

V_{Wind} : Wind speed (m/s)

α_{th} : Coefficient of thermal expansion

ϵ_m : Mechanical strains

ϵ_{th} : Thermal strains

μ_l : Coefficient de frottement longitudinal

φ_{conv} : Coefficient of longitudinal friction (W/m^2)

S_{br} : Braking surface (m^2)

t_{br} : Braking time (s)

A: Temperature range (˚C)

D: Thermal diffusivity of the layer (m^2·s^{-1})

k: Thermal conductivity (W·m^{-1}·K^{-1})

Lx: Length of the pavement (m)

M: Vehicle mass (kg)

p: Slope of the pavement's longitudinal profile

T: Temperature (˚C)

t: Time (s)

α : Albedo of the pavement surface

ϵ : Emissivity of the pavement surface

ρ : Density (kg·m^{-3})

σ : Stefan-Boltzmann constant 5.669 × 10^{-8} (W·m^2·K^{-4})

φ : Phase

E: Modulus of rigidity (Pa)

e: Thickness of the layer (m)

v: Poisson ration

τ : Period of daily fluctuations (s)

ω : Daily pulse (s^{-1})

v: Vehicle speed (km/h)

D_{br} : Braking distance (m)